FRAGBLAST – International Journal of Blasting and Fragmentation 1(1997): 3–25

Monitoring of large open cut rounds by VOD, PPV and gas pressure measurements

F. Ouchterlony, S. Nie, U. Nyberg & J. Deng

Swedish Rock Engineering Research, SveBeFo, Stockholm, Sweden
Tel: +46-8-6922280, Fax: +46-8-6511364, E-mail: rock.engineering@svebefo.se

ABSTRACT: A project with the goal to minimize the blast damage to the remaining pit walls has been carried out at the Aitik open pit mine in North Sweden. Factors like confinement during the blast, blast direction and size of blast holes in the contour were systematically changed. During the blasts VOD in the blast holes plus PPV and gas pressure in gauge holes behind the contour were monitored.

The VOD measurements were used to check the explosive performance, to obtain the real initiation sequence and to identify the sources of the PPV pulses in the composite acceleration records. The PPV levels were used to establish a scaling law for the test area which later was used for blast damage assessments.

The gas pressure measurements show that the ordinary rounds don't force any significant amounts of high pressure blast fumes into the walls, probably because the unstemmed blast holes allow venting of the fumes.

In all gauge holes behind ordinary rounds, only subatmospheric pressures were recorded. This is probably explained by a shock wave initiated dynamic swelling movement that opens up fractures. Those fractures that are or become connected with the gauge hole increase its volume and reduce its pressure. The measured underpressures correlate relatively well with the measured residual swell values.

The fracture dilation velocity is estimated from the maximum pressure drop rate in the pressure-time records. It lies in the range 0.05–2.0 m/s and it is considerably smaller than the swelling rate as given by the measured PPV-values. Further a shot pre-split line didn't transmit direct shock waves or blast fumes into the walls. The pre-split blast holes themselves though, despite being unstemmed, did however force pressurized blast fumes into the rock. Thus, they may be a source of blast damage.

KEYWORDS: open pit mine contour blasting, blast damage, pre-split, VOD, PPV, gas pressure, swelling.

1 INTRODUCTION

The Boliden Mineral AB, Aitik open pit copper mine in North Sweden, see Figure 1, produces about 15 Mton of 0.4% grade ore annually. The slope conditions are of vital importance to the mine economy, hence the strong requirements to reach the planned interramp and bench face angles. Even if geology determines the stability to some extent, the blast damage may be quite important for the individual bench crests and have large economic consequences.

Figure 1. Photo of Aitik mine, facing north with foot wall on right hand side and test area below plant.

The mine uses double 15 m benches with a catchment berm every other level. The berm has to be at least 11 m wide over 90% of its length for it to function properly. This was not always so and projects were initiated to deal with it, the first in 1991 (Sognfors 1994, Siira 1994). Despite a steepening of the bench angles, the blast damage to the walls still seemed to be large. Thus a more pronounced cautious blasting of the final slope seemed motivated.

Phase 2 started in 1993 with Boliden as coordinator and with SveBeFo and Nitro Nobel as partners. Field tests were made during late fall and early winter of 1993.

Two production rounds were divided into smaller rounds while varying the following factors:

- the degree of confinement of the round, i.e. the number of rows fired,
- the direction of mass movement through variations in the drilling and ignition plan, and
- the use of either the larger production holes ($12\,1/4'' = 311$ mm) or the smaller contour holes ($5\,1/2'' = 140$ mm) in the last row of the round.

Pre-splitting of the contour was also tried as a complement to the smooth blasting usually used.

A monitoring program was set up with the purpose of showing how backbreak and other forms of blast damage are influenced both by the blasting itself and by the geology. It had three parts:

- careful documentation of drilling, charging and the laying out of the firing lines,
- measurement of VOD, PPV and air pressure in the slope behind the contour holes, and
- measurement of the back break and crest profiles in the contour plus the vertical swelling of the bench and the round.

An evaluation of the tests later led to recommendations to the mine on how to conduct its contour blasting.

This paper focuses on the blast monitoring. Its purpose was to check that the explosive in the blast holes detonates with the correct VOD, in the right sequence and with the proper delay. Furthermore

1. The VOD-records were used to identify which blasthole was the source of what PPV-pulse.
2. The PPV-records were used to construct the site scaling laws needed for damage zone evaluations.
3. The measurement of gas/air pressure in empty bore holes was used both to determine the contribution of the blast fumes to the damage in the remaining bench face and to study the effect of the pre-split crack in protecting the face from PPV pulses and gas penetration.

The work by LeJuge et al. (1994) was a very helpful starting point for our gas pressure measurements. Such measurements have also been made by Armstrong (1987), Sarma (1994) and Brent & Smith (1996). Our pressure measurements have been presented to an international audience (Ouchterlony 1995, Ouchterlony et al. 1996).

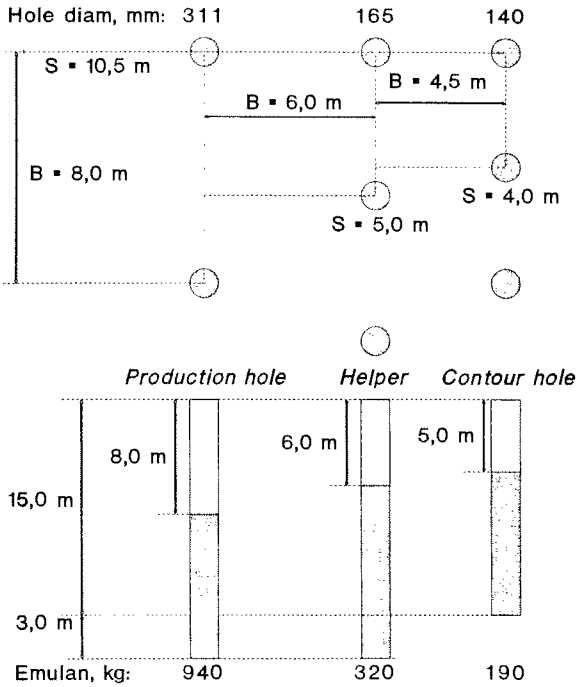

Figure 3. Ordinary drilling and charging pattern on foot wall.

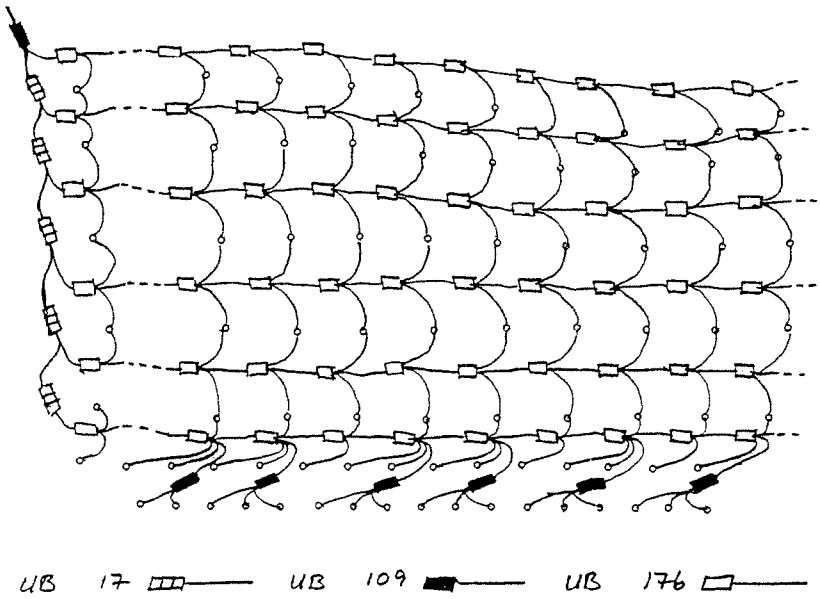

Figure 4. Nonel Unidet initiation on foot wall.

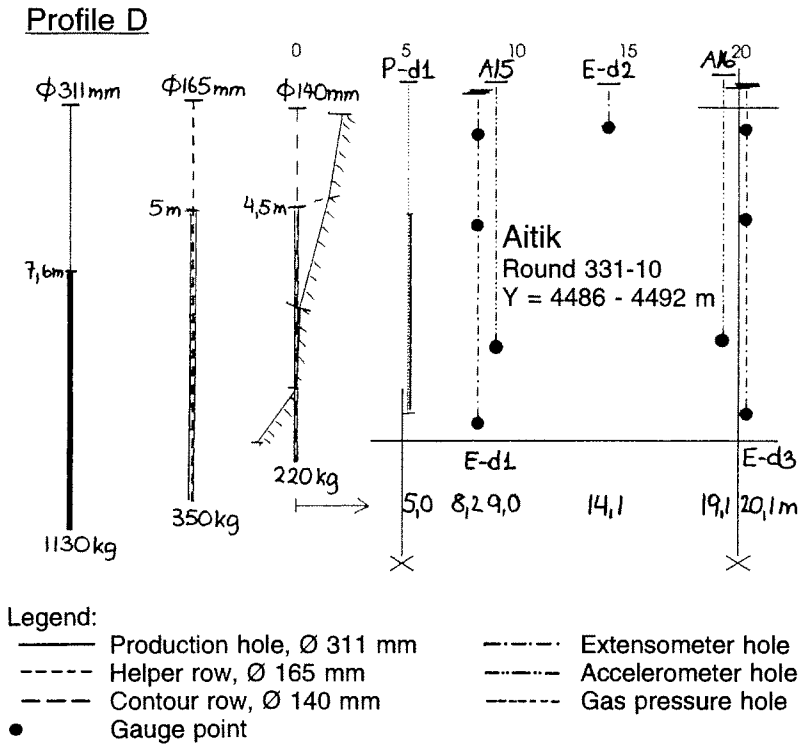

Figure 5. Instrumentation profile D, round 331-10.

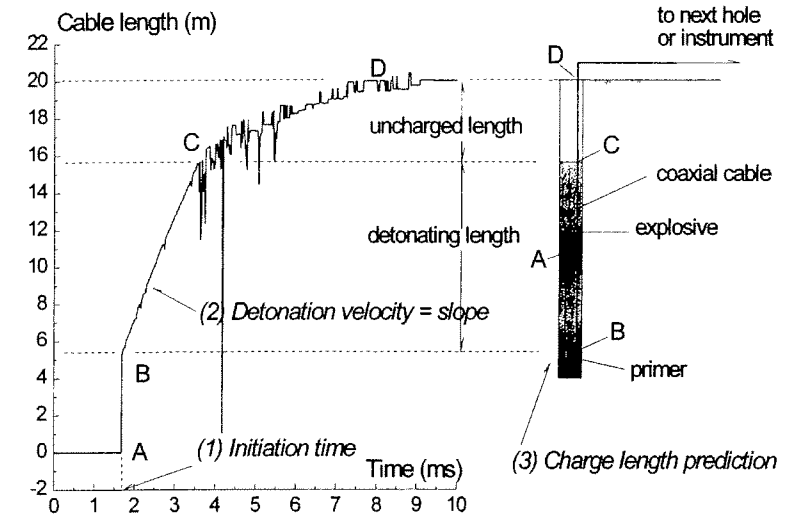

Figure 6. VOD registration, i.e. movement of shorting point in coaxial cable for hole 1 in round 330-1.

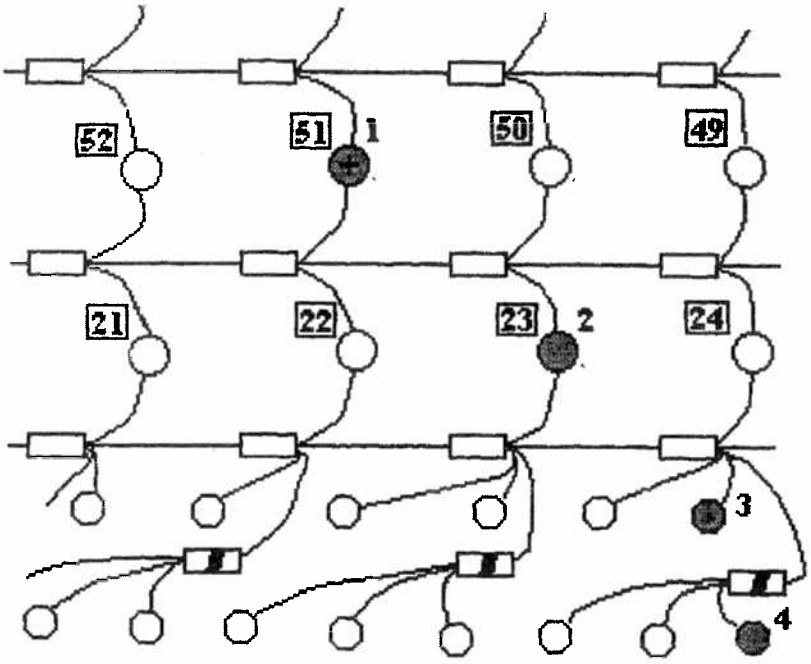

Figure 7. VOD holes outside profile D in round 331-10.

Figure 6 shows a recording of the position of the detonation front with time. The pigtail part AB is instantaneously shorted by the primer, the slope of part BC gives the VOD in the charge and CD shows the movement of a pressure wave or the blast fumes through the empty unstemmed part of the bore hole.

Figure 7 shows how the instrument was used to measure the relative initiation times of holes in 3 trunk lines and the contour row outside instrumentation profile D.

2.3 *PPV measurements*

The relevant part of the ground vibration event is the peak particle velocity at the front of the shock wave which emanates from a detonating charge. This value, the PPV, is often used as an engineering measure of the loading to which the material is subjected and consequently as a means to evaluate the blast damage (Holmberg & Persson 1979).

Close to a blast hole, it is our experience that the frequencies are well above 1 kHz so we prefer to use accelerometers. At Aitik the ground vibrations were measured at the bottom of 12 m deep ∅165 mm holes, approximately at the same level as the center of gravity of the production charges, see Figure 5.

The gauges were mounted on a base plate with a threaded stud, see Figure 8, which was attached to the end of a string of ∅63 mm PVC pipes. Thus we could insert the gauges into the hole before measurements and remove them afterwards while protecting them from moisture. The base plate stud fits into a conical foot which had been securely grouted in place with expanding, quick curing and freeze

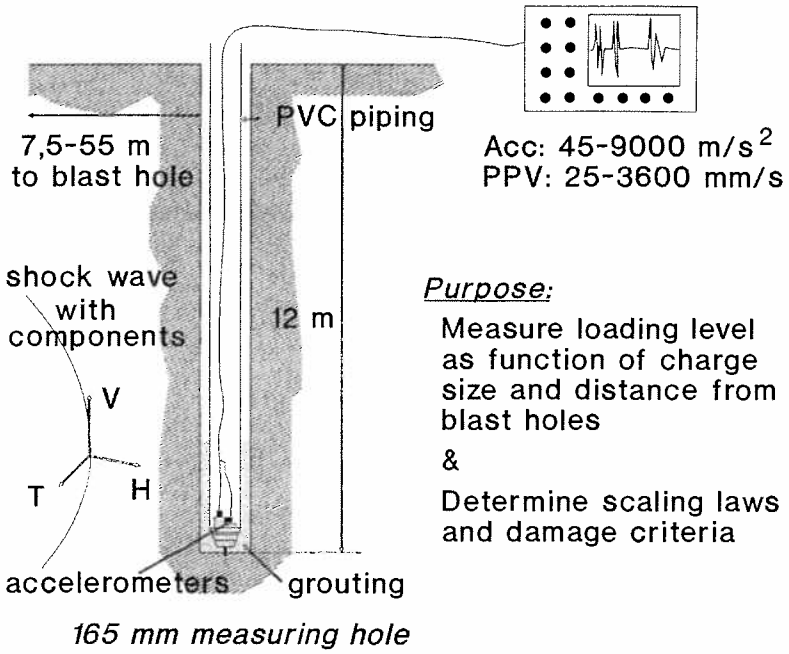

Figure 8. Gauge hole for PPV measurements with accelerometers.

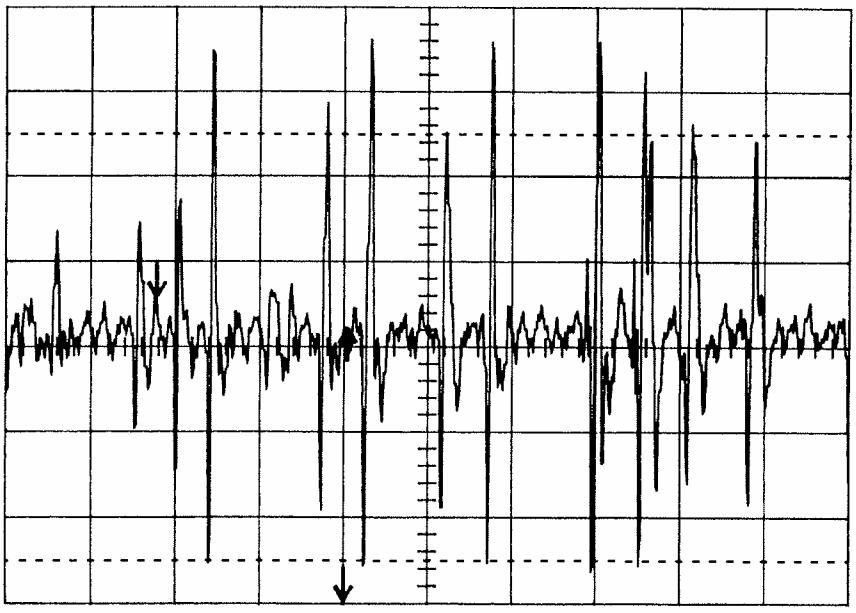

Figure 9. Vertical acceleration, hole A-20 in profile G, round 331-10, max 285 m/s^2. x-axis: 100 ms / square.

resistant cement. The mount in turn was protected by a PVC pipe sleeve which made it possible to screw the base plate to the foot from the surface.

The measuring system consisted of accelerometers, charge amplifiers and recording units for a maximum of 16 channels. The accelerometers were of type Brüel & Kjaer 2635 or 2626 with a 12.5 kHz bandwidth. The recording units were one 14 channel FM tape recorder TEAC XR-510 with 20 kHz bandwidth and one 6 channel digital recording unit with a 6 kHz bandwidth and a 10 s storage window. Whenever possible channels were doubled and in each instrumentation profile there were at least two sets of 2 or 3D accelerometer assemblies, see Figure 5.

A trace is given in Figure 9. It shows that it may be quite difficult to match each pulse in the round with the correct source. We used both ionization probes and the VOD records to do the matching.

2.4 *Gas/air pressure in bore holes measurements*

All gas/air pressure measurement holes except one were vertical, 15 m deep and had ∅165 mm. The damaged upper part was sealed off by a ∅110 mm, 6 m long capped plastic pipe, Figure 10.

The gauge was mounted in the cap under extra protection. In the gauge output, a DC level represented atmospheric pressure, so there was no mistaking a nonresponding live gauge for a dead one.

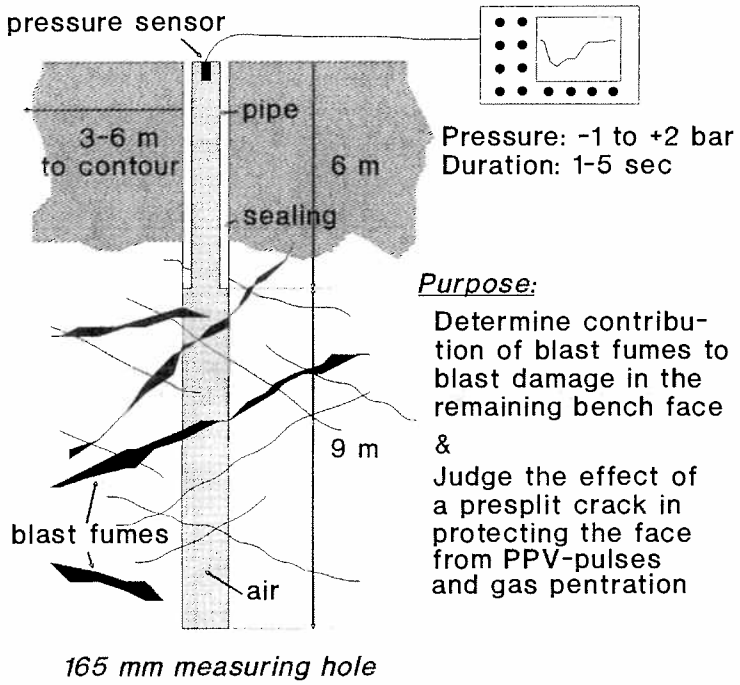

Figure 10. Sealed holes for gas/air pressure measurements.

The pressure gauges were of foil strain gauge type, Haenni model ED 517/314.211/075. They had a range of 0–10 bars because we expected mainly over-pressures from the pressurized blast fumes that would penetrate the cracks in the slope. The holes were positioned 3–25 m behind the contour. Pressure measurements were made in 9 of the instrumentation profiles, each using 1–3 holes. Signals were obtained from 17 out of 18 holes and from all profiles.

3 RESULTS AND INTERPRETATIONS

3.1 *VOD results*

The VODR-1 worked well even in the wet subfreezing conditions. Data are given in Table 2. From 46 instrumented holes, 44 initiation times were obtained and from these 35 good VOD versus time histories were obtained. Four of the missing ones came from the pre-split rounds 331-8+9 where the interhole delay was 1 ms.

The VOD values were as expected, being highest near the primer and decaying towards the top of the holes, as the density of the explosive decreased. The VOD values of the production holes were about 10% higher than for the smaller holes. The differences between the VOD values of the ∅140 and ∅165 mm holes were however too small to be significant compared to the scatter, which was about 5–10%. This shows that the explosive held a consistent quality during our tests. The VOD recordings could also be used to judge the charge length with acceptable accuracy, but not the uncharged length.

Table 2. Summary of VOD-values.

Round no	∅mm – no holes	VOD bottom m/s	VOD top m/s	VOD average m/s
330-1	311 – 3	5750–6180	4650–5380	5200–6500
330-2	311 – 1	6550	5880	6080
	165 – 2	5530–5800	4250–5090	5000–5230
	140 – 2	5440–5600	4210–4570	4920–5140
330-3	311 – 4	6060–6110	4700–5590	5460–5890
331-5+6	311 – 6	5940–6740	4160–5650	5310–6220
	165 – 1	5620	3950	4530
	140 – 1	6320	3580	4900
330-4+331-7	165 – 1	5810	5170	5430
	140 – 2	5870–5890	4930–4980	5300–5550
331-8+9	140 – 2	4930–5130	4200–5160	4500–5170
331-10+11	311 – 7	5680–6710	4770–5420	5490–6080
	165 – 3	5420–5690	3600–5560	4230
	140 – 1	5690	5030	
Total	311	6200 ± 300	5200 ± 400	5700 ± 300
	140–165	5600 ± 300	4600 ± 600	5100 ± 400

Figure 11 shows the relative delay of the initiation time of the holes along a VOD cable with respect to the previous hole, divided by the nominal scatter of the relevant delay elements and caps. The values should simplistically be normally distributed with a standard deviation of 1 around the average value 0.

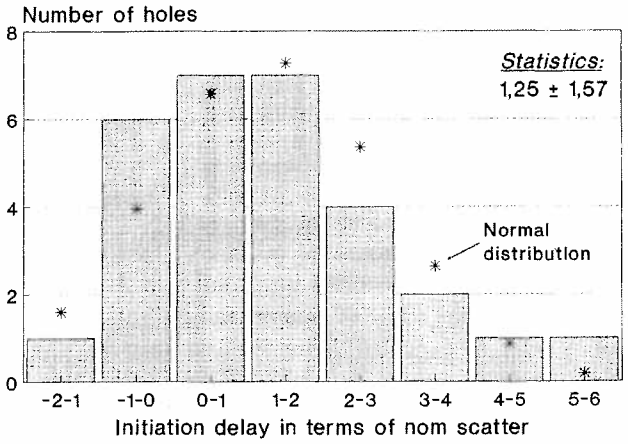

Figure 11. Relative delay in initiation of VOD measurement holes in rounds 330 and 331.

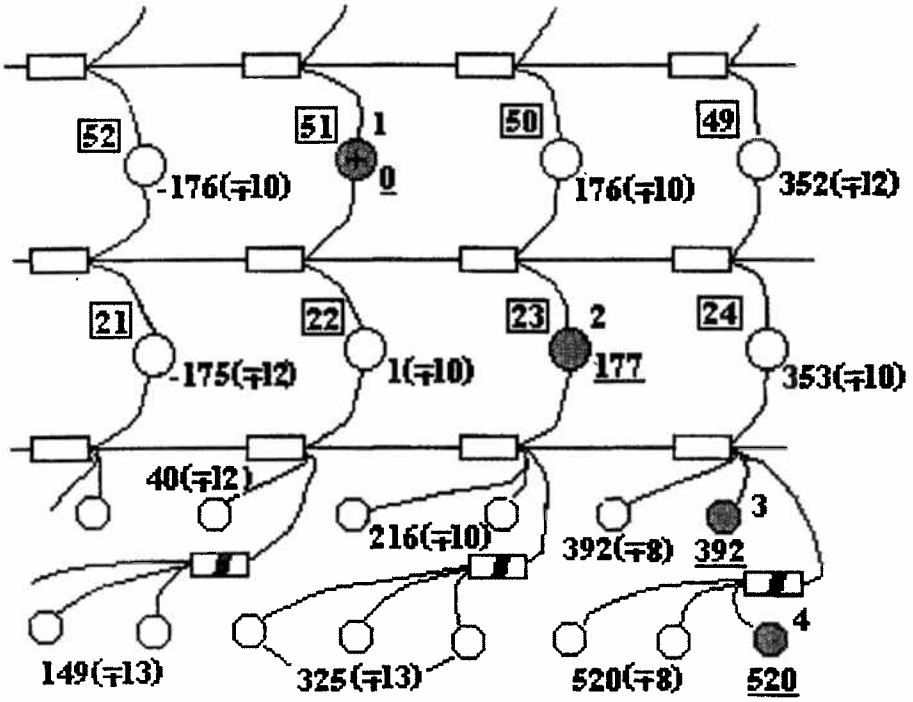

Figure 12. Measured and predicted initiation times in round 331-10, relative to hole no 51.

The actual average 1.25 can be explained by the additional 12.5 ms delay of the initiation impulse as it propagates down about 25 m of shock tubing at 2000 m/s. The actual standard deviation 1.57 is probably an RMS build up of individual scatters.

Figure 12 shows the VOD holes outside instrumentation profile D, cf. Figure 7. The underlined numbers 177, 392 and 520 show how late after hole no 51 the real initiation occurred. The number 1(∓10) for hole no 22 is a back calculation from hole no 23, considering the initiation time scatter of delay element and cap.

According to Figure 7, hole no 22 should have been initiated 17 ms after no 51 but in reality they were initiated nearly simultaneously. The same then was true for hole pairs 52–21 etc. This shows the difficulty to identify the true sources of the shock wave pulses in a recording like Figure 9, using only the initiation pattern. Despite the example above, there were no specific complaints on the initiation sequences of the test rounds by production people.

3.2 *PPV results*

PPV was measured in 11 of the 16 instrumentation profiles using 2 gauge holes each. Three-dimensional gauges were used in all rounds except the last one where the vertical and horizontal components along the profile were measured. Signals were obtained from 17 of the 22 gauge holes and from all profiles. The scatter in the amplitudes and the absence of a dominating component made vector evaluation unnecessary so all results refer to velocity components.

These components were plotted in synthetic PPV profiles like the one for instrumentation profile D in Figure 13. Here all identifiable ∅140 mm sources have been moved to the contour position, all identifiable ∅160 mm sources to the helper row position 4.5 m out and all ∅311 mm sources to the first production row another 6 m out from the helper row.

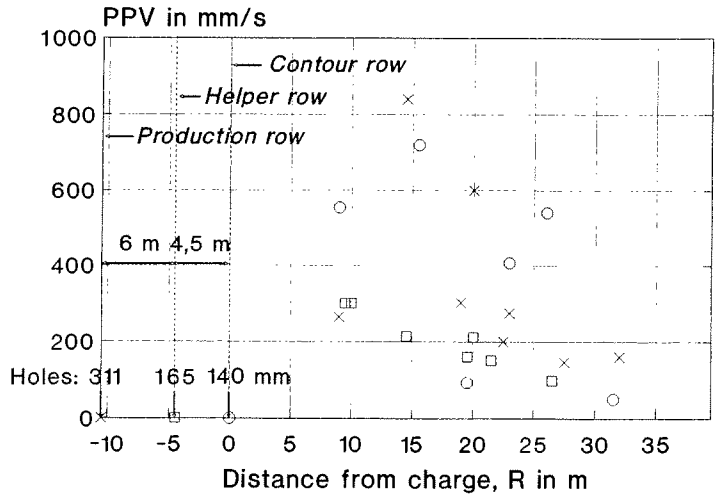

Figure 13. Synthetic PPV profile for instrumentation profile D, nominal burdens 4.5 and 6 m.

The quality of the results was sufficient to determine site scaling laws. The swelling in the bench could however not be obtained with sufficient accuracy from the vertical acceleration through a double integration.

3.3 *Gas/air pressure results*

The gas/air pressure measurements are summarized in Table 3. A clean pressure signal from an ordinary round is shown in Figure 14. Here the pressure usually starts to drop before the closest charged hole detonates, as indicated by negative arrival times in Table 3. We had expected overpressures to occur but in 10 out of 13 holes there are only underpressures like in the figure. In one case a cable was

Table 3. Air/gas pressure measurement data; gauge distance from closest blast hole, peak pressure, duration, arrival time, max pressure drop rate, and fracture dilation rate.

Round/ profile no	Distance m	Peak pressure atm	Duration s	Arrival time ms	Maximum drop rate bar/s	Dilation rate m/s
330-3/I	11.7	−0.28	3.7	12	3.64	0.38
330-3/I	21.8	±0	–	–	–	–
330-3/I	24.6	±0	–	–	–	–
330-4/I	2.9	−0.62	1.3	–	6.35	2.00
330-4/I	5.7	−0.39	2.6	–	2.16	0.30
330-7/B	4.6	−0.62	1.1	−147	4.90	1.55
330-7/B	2.6	−0.21	>0.5	−87	1.52	0.14
330-7/B	6.3	−0.22	5.3	−70	1.80	0.17
331-8/C	3.0	+1.77	1.3	3	7.69	0.66
331-8/C	5.6	±0	–	–	–	–
331-9/E	2.8	+1.60	4.5	7	–	–
331-9/E	6.4	+0.19	12.2	9	0.75	0.05
331-10/D	5.0	−0.31	2.5	−2420	1.37	0.16
331-10/E	5.1	±0.08	–	–	–	–
331-10/E	7.7	–	–	–	–	–
331-10/G	6.1	−0.27	1.3	−288	2.00	0.21
331-10/G	12.3	−0.37	1.2	−17	2.54	0.34
331-11/F	3.5	−0.47	1.8	−344	3.80	0.68

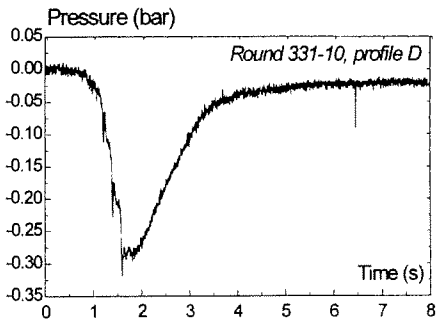

Figure 14. Air pressure in gauge hole P-d1, 5 m behind contour in round 331-10.

cut and from the two farthest gauge holes, 22 and 25 m respectively, we measured insignificant pressure variations.

This underpressure is probably caused by the vertical movement in the rock which the shock fronts from the charges initiate and which is amplified by the reflections from the top surface of the bench. This swelling opens up fractures connected to the measuring hole, increasing its effective volume. The pressure drops when the air in the hole is sucked into the fractures. The hole and the fractures behave roughly like an 'accordion' together.

The pressure equilibrium is restored as air and maybe blasting fumes flow into the hole. We can not exclude the possibility of the blast fumes from entering the hole, but if so, their pressure effects are negligible. The durations of these pulses were 1–5 s and the maximum underpressure measured was about 0.6 bar 3–4 m behind a charge. This pressure decrease would require a doubling of the original hole volume.

During our pre-splits two gauge holes at roughly 3 and 6 m behind the charge line were used in each of the profiles C and E. Three of them returned measurable levels, the remaining one a negligible level. All three show the same behavior, see Figure 15. After a short negative pulse (< 0.2 bar except for noise spikes) the pressure rises fast to a substantial overpressure, between 1.6–1.8 bar 3 m behind the split.

What sets the pre-splits apart from ordinary rounds is the confinement of the surrounding rock and that the 1 ms delay in charge initiation allows the charges in adjacent holes to cooperate. This appears to be enough to force blast fumes into the remaining rock. This penetration may in parts have been helped by open fractures parallel to the foliation.

The effect of the pre-split was to be judged by 2 gauge holes in instrumentation profile E but the only signal came from 1 m behind the uncharged pre-split or about 5 m behind the charged ∅165 mm holes.

Figure 16 shows that the pre-split effectively cuts off the pressure, compared with hole D1 which is situated just as far behind a charged contour row, cf. Figure 5.

The PPV measurements indicated the same effect on the incident shock wave. However, the damage may already be there since pressurized blast fumes have penetrated the rock mass during the pre-split.

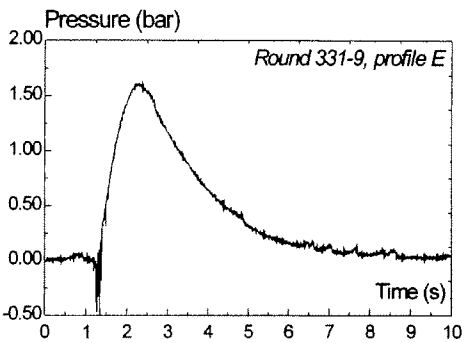

Figure 15. Pressure in gauge hole P-e2, 2.8 m behind pre-split line in pre-split round 331-9.

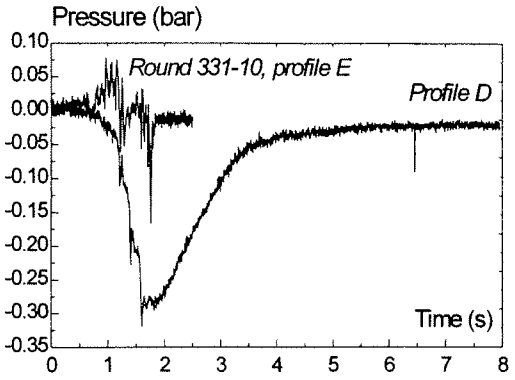

Figure 16. Pressure in gauge hole with (E1) or without a pre-split crack shielding the charges.

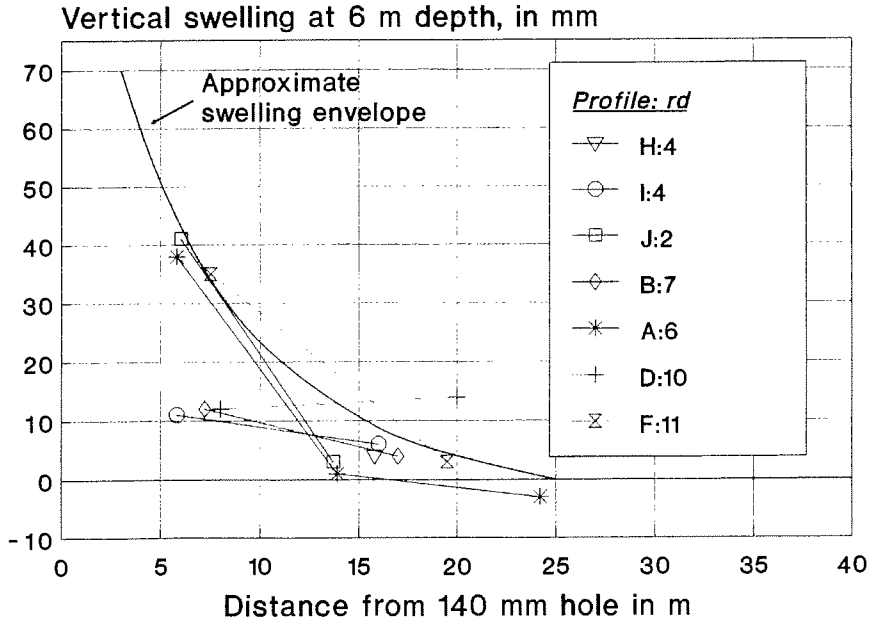

Figure 17. Vertical swelling behind ∅140 mm blast holes, as measured by extensometers anchored at 6 m depth.

The vertical swelling, h, in the bench after blasting can go more than 20–25 m in from the blast holes as may be seen in Figures 17 and 18. If we assume that it is due mainly to an irreversible dilation of the fractures during the round we can relate it to the measured underpressures. Since the upper 6 m of the pressure holes were sealed off, it follows that the extensometer readings at 6 m depth below surface are a measure of the fracture widths accumulated below it. The active hole length $H \approx 9$–10 m.

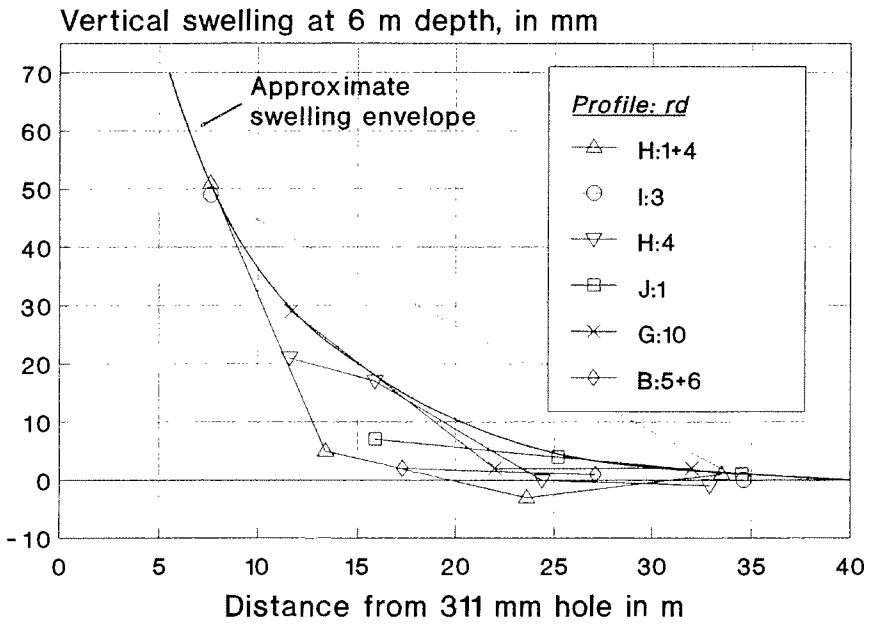

Figure 18. Vertical swelling behind ∅311 mm blast holes, as measured by extensometers anchored at 6 m depth.

For simplicity assume: i) that these fractures can be represented by a number of circular fractures of radius R, ii) that the deformation of the rock mass is small compared to the relative displacements of its blocks and iii) that the air in the hole follows a polytropic gas law. The time it takes to fill a crack of length $R \approx 1$ m with air is of the order 10 ms. The time for the pressure drop in our records like Figure 14 is usually 150–300 ms, sometimes more. As an engineering approximation we can thus assume iv) that the process is quasistatic.

For the gas volume V in the sealed monitoring hole, thus

$$p \cdot V^{\gamma} = p_o \cdot V_o^{\gamma} = \text{constant} \quad \text{and} \tag{1}$$

$$V = V_o + h \cdot \pi R^2 \quad \text{with } V_o = \pi \varnothing^2/4 \cdot H \tag{2}$$

It follows with $p_o = 1$ atm that

$$p_{\min} \approx 1/\left[1 + 4(R/\varnothing)^2 \cdot (h/H)\right]^{\gamma} - 1 \tag{3}$$

Like the PPV-data, the swelling data scatters much but the envelopes for the two main hole sizes, ∅140 and 311 mm, give upper limits, see Figures 17 and 18. The right magnitude for 2R would be somewhat larger than the average distance between fracture planes, 0.9–1.7 m. With $2R = 1.8$ m and $\gamma \approx 1.4$ for air we get the results in Table 4 and Figure 19.

Since swelling envelopes were used, the pressure curves should envelope the measured values in Figure 19. This they do reasonably well so the agreement is acceptable and this supports the hypothesis that the measured underpressures in the holes are due mainly to the opening of fracture planes in the rock mass.

Table 4. Estimated underpressures in gauge holes.

Swelling mm	Pressure atm	Distance to ∅140 m	Distance to ∅311 m
70	−0.57	3.0	4.5
50	−0.48	5.0	7.1
30	−0.35	8.2	11.5
20	−0.26	11.0	15.1
15	−0.21	13.0	17.2
10	−0.15	15.2	20.1
5	−0.08	18.2	25.0

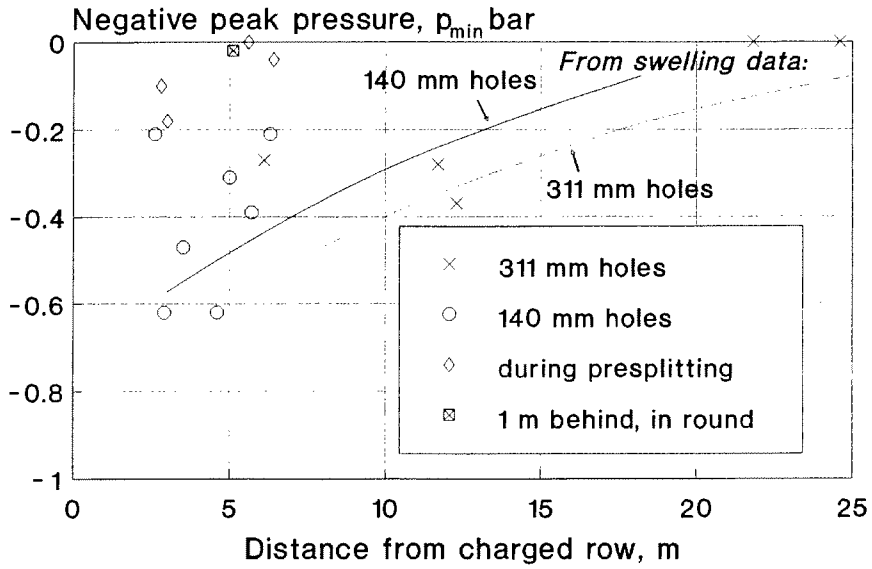

Figure 19. Measured underpressures and pressure estimates based on Equation 3 and data in Table 4.

Then a further development is possible. Equation 2 may be differentiated with respect to time and V eliminated to obtain the fracture dilation velocity dh/dt,

$$dh/dt = H/\gamma \cdot \left[- d(p/p_o)/dt \right] \cdot (\varnothing/2R)^2 \cdot (p_o/p)^{1+1/\gamma} \quad (4)$$

The rate of pressure drop $-d(p/p_o)/dt$ can be read from the pressure-time records and the use of $p \approx p_{min}$ in Equation 4 gives an upper limit estimate of dh/dt.

The pressure drop rates and the calculated fracture dilation velocity values are given in Table 3. The individual dilation velocity values range from 0.05–2.0 m/s, see Figure 20. They will be compared with the PPV-values in section 3.5 below.

3.4 *Comparison with other pressure measurements*

Brent & Smith (1996) report gas pressure measurements in 14 monitoring holes 7–25 m behind limits for four bench blasts in sandstone with ∅200/270 mm holes.

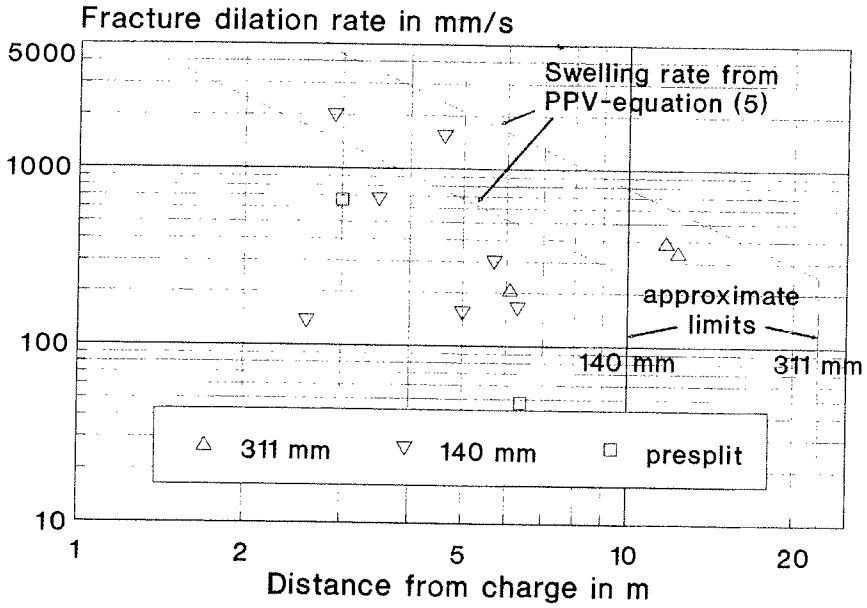

Figure 20. Fracture dilation velocity below 6 m depth, calculated from measured pressure drop rates and Equation 4.

Underpressures were consistently recorded. In one blast 4 holes were drilled and mapped pre- and postblast with a bore hole video camera.

Even if there were no obvious visible structures or discontinuities before the blast, many large open cracks could be seen afterwards. They were mostly horizontal, some were vertical. The extent of cracking was more pronounced near the surface and decreased with the distance behind the blast limit. The widths of these cracks were in the range 5–75 mm and the aperture areas (width · length) correlate well with the measured peak underpressures which go down to −0.78 atm.

They also monitored 2 fully confined crater blasts, each with a single 10 m deep ∅89 mm hole. They used 4 monitoring holes between 1–8 m away in each blast. Their pressure signals look basically like our pre-split signal in Figure 15, an initial underpressure (in some cases) and then a major overpressure pulse with a maximum of up to 2.8 atm.

Summing up, the observations of Brent & Smith (1996) are remarkably consistent with ours. They reach basically the same conclusions regarding what causes their measured under- and overpressures. They substantiate our 'accordion effect' explanation above and add to it in that the fractures that open could both be ones that exist before the blast and ones that are created during it. They obtain characteristic crack depths, corresponding to R in Equation 2, of the order of meters etc.

Our observations are also largely in agreement with those of LeJuge et al. (1994) from the Rössing mine. They attribute the underpressure to the same mechanism as we and they didn't detect any gas flow across their pre-split crack either.

Behind a stemmed pre-split blast they measured a signal much like Figure 14 at 2 m, but with a shorter duration. At 4 m the overpressure had decayed substantially

and at 6 m the initial negative pulse dominated completely. The difference might be caused by their more lightly charged pre-split, about 18 kg per hole vs our 90 kg, and a more fractured rock which would both exaggerate the fracture dilation effect and shorten the pressure restoration time.

The pressure record they show from a ∅381 mm, 15 m deep stemmed production hole is different from Figure 14 though. At 5 m they recorded a substantial over-pressure, something which we never found behind our unstemmed Aitik production holes.

We can probably attribute this to the pressure retaining effect of the stemming at Rössing. It then follows that an unstemmed blast hole is important in venting the blast fumes and avoiding gas penetration into the rock mass. For the Aitik mine at least, we were able to conclude that the blast fumes from an ordinary unstemmed blast in all probability don't give a significant contribution to the blast damage.

However, it doesn't necessarily follow that:

– the blast damage would be measurably smaller if there were no stemming, nor that,

– the stemming effect which contains the blast fumes would significantly add to the damage.

Firstly, the swelling goes considerably deeper than the gas penetration, compare Figures 17 and 18 with Figure 19, and all fracture dilation should be considered as damage once it has reached a certain level, no matter what caused it. Secondly, we have made no comparative experiments where the stemming is the only test variable.

Hommert et al. (1987) have however reported a heavily instrumented comparison between two identical crater blasts in oil shale, one stemmed and one unstemmed. The holes were 5 m deep with ∅165 mm and 2.5 m of explosive at the bottom. Based on their observations and simulations they conclude that the absence or presence of stemming has no impact on the extent of rock fracture as defined by mean fragment size or extent of fracture.

3.5 *The site scaling laws*

The synthetic PPV profiles, like in Figure 13, give a good idea of how the measured PPV-values depend on distance R (m), charge size Q (kg) and charge length H (m). They show how far into the wall waves of a certain amplitude can penetrate. The present Aitik data could be divided into two groups, mainly the foot wall profiles and those parallel to the wall.

A site scaling law was fitted to the complete set of foot wall data,

$$\text{PPV} = 160 \cdot \left(\sqrt{Q/R}\right)^{1.42} \quad \text{in mm/s} \tag{5}$$

The prefactor for our profiles varied between 130 and 220. The uncertainty in A could also be expressed through the standard deviation factor 2.03. The equation and some of the data are shown in Figure 21 together with an upper limit line. Previously measured PPV data follow this trend well too, see Figure 22.

If we let the PPV data represent the swelling rate, we can plot Equation 5 with the charge weights of Figure 3, 190 kg for the ∅140 mm holes and 940 kg for the ∅311 mm holes, in Figure 20. Here the fracture dilation rate (velocity) usually falls below, perhaps by a factor of 4. The main reason for this may be that the total

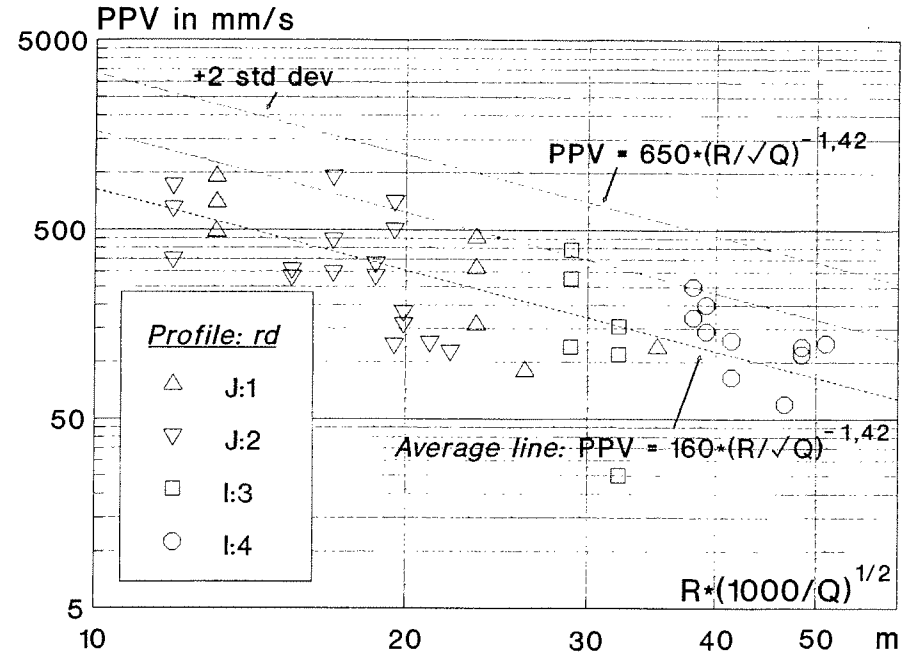

Figure 21. PPV data from instrumentation profiles I and J, rounds 330-1 to 4.

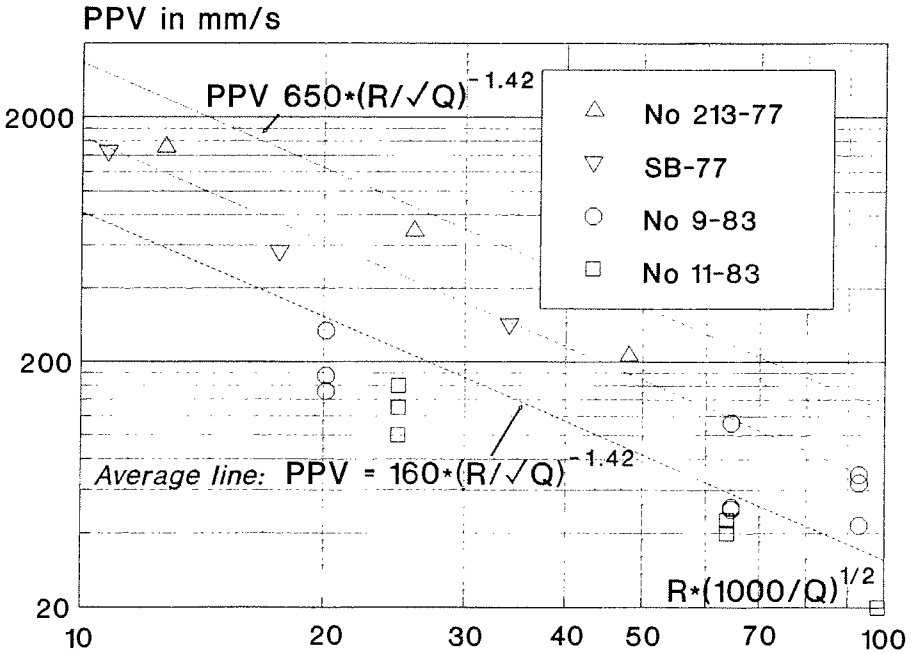

Figure 22. PPV data from old Aitik measurements.

swelling rate contains both the fracture dilation rate and in addition elastic and rigid body velocity components.

The different PPV-data for instrumentation profiles oriented along and across the foot wall made us estimate the wave propagation velocity parallel and perpendicular to the foot wall. We combined the VOD initiation time and the PPV arrival time data with the distance between source and receiving gauge to obtain a P-wave speed of 4850 m/s independently of direction.

Scaling laws of the form (5) predict the average PPV value as a function of charge size and distance. In estimating the depth of a blast damage zone we are perhaps more interested in obtaining engineering estimates of their maximum penetration. Ouchterlony et al. (1993) handled this by using a double deviation factor for A. If the errors are random and normally distributed, 98% of the measured values should fall below this limit.

Close in, only part of the charge is expected to contribute to the PPV value (Holmberg and Persson 1979). Adding this charge length correction to Equation 5 we obtained the following limiting curve for the PPV values in the foot wall

$$\mathrm{PPV} = 650 \cdot \left[\sqrt{(fQ)/R}\right]^{1.42} \quad \text{in mm/s} \quad \text{with} \tag{6a}$$

$$f = \left[\mathrm{atan}(H/2R)/(H/2R)\right] \tag{6b}$$

In Figure 23 all the foot wall data are shown together with the limiting curves for the different holes. Close to the final wall, the contour holes dominate the loading but already 8–9 m into the wall the production holes start to dominate. The ∅165 mm

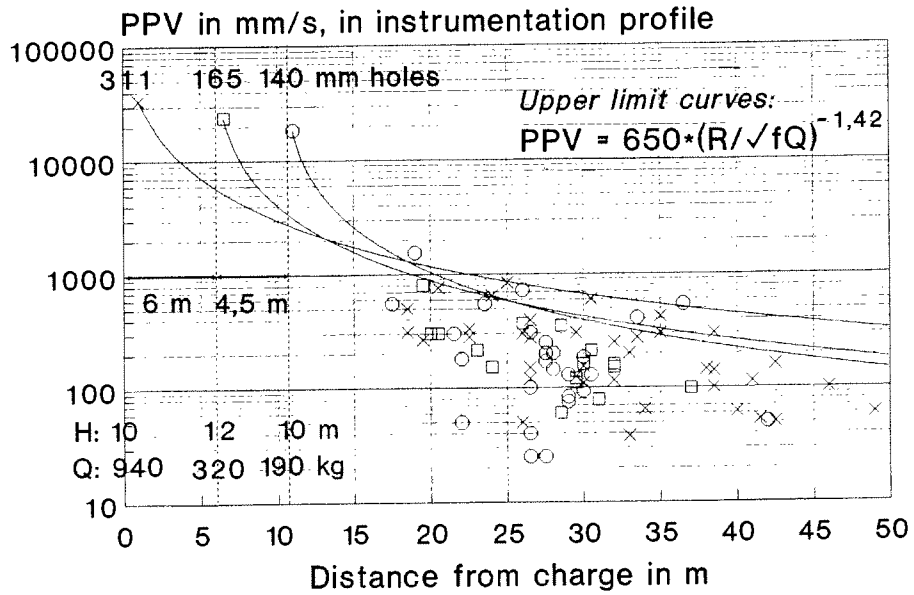

Figure 23. Synthetic PPV profile for foot wall, including data and Equations 6.

holes seem to be relatively harmless though, which leaves room for an improved blasting pattern with balanced PPV-levels.

4 CONCLUSIONS

Based on the monitoring results from the Aitik mine test blasts, the following conclusions could be drawn:

– VOD is an excellent means of checking the performance of explosives and initiation system in a blast. At Aitik both of these worked well.

– At Aitik the VOD records were instrumental in pin pointing 10–20 individual PPV pulse sources in each round.

– The charges in ordinary rounds, in which the blast holes are unstemmed, didn't force any significant amounts of high pressure blast fumes into the walls since only subatmospheric pressures were measured.

– A shock wave initiated dynamic swelling movement opens up fractures. Those fractures that are or become connected with the gauge hole increase its volume and reduce its pressure. The measured underpressures correlate relatively well with the measured residual swell values.

– The pressure drop rates from the pressure–time records could be used to estimate the fracture dilation velocity which is considerably smaller than the measured PPV-values.

– The shot pre-split line didn't transmit direct shock waves or blast fumes into the slope. The pre-split holes themselves did however, despite being unstemmed, force pressurized blast fumes into the rock.

Despite their relatively confined conditions, the blast fumes from normal blast holes could thus be eliminated as a direct source of blast damage. This doesn't rule them out as a considerable source of damage if the holes are stemmed so that the blast fumes are prevented from venting axially.

The blast damage assessment which followed could thus focus on the PPV levels. Measurement of back break and swelling made it possible to quantify different blast damage zones and, through the scaling law, to relate it to the blasting patterns. This has been the basis for suggested designs of cautious blasting that the mine has been trying out. The results of this part of the project will be reported later.

ACKNOWLEDGEMENTS

The authors thank Boliden Mineral AB for the permission to publish this work. The efforts of the Aitik mine staff, especially Karl Johan Eriksson, blasting and Olavi Siira, planning are gratefully acknowledged. Our thanks also go to the project group under the leadership of Per-Olof Sognfors. Boliden engineer Staffan Sandström made the extensometer measurements and Norbert Krauland was responsible for rock mechanics matters. Roger Holmberg, Nitro Nobel and William Hustrulid, LKAB both contributed their considerable expertise. Dr Anders Dahlkild of the Royal Instute of Technology, KTH in Stockholm is acknowledged for his contribution to Equation 4.

REFERENCES

Armstrong, M.E. 1987. The measurement of gas penetration from an explosive charge. M. engng sci. thesis. Brisbane QLD: Univ. Queensland.

Brent, G.F. & Smith, G.E. 1996. Borehole pressure measurements behind blast limits as an aid to determining the extent of rock damage. In B. Mohanty (ed.), *Rock Fragmentaton by Blasting, Proc. 5th International Symposium*: 103–112. Rotterdam: Balkema.

Chiappetta, R.F. 1993. Continuous velocity of detonation measurements in full scale blast environments. In P. Weber (ed.), *Rock Blasting, an International Summer Seminar*: 27–74. Alès: Ecole des Mines.

Holmberg, R. & Persson, P.-A. 1979. Design of tunnel perimeter blasthole patterns to prevent rock damage. *Proc. Tunnelling '79*: 280–283. London: Inst. Mining and Metallurgy.

Hommert, P.J., Kuszmaul, J.S. & Parrish, R.L. 1987. Computational and experimental studies of the role of stemming in cratering. In W.L. Fourney & R.D. Dick (eds), *Rock Fragmentation by Blasting, Proc. 2nd International Symposium*: 550–562. Bethel, CT: SEM.

LeJuge, G.E., Jubber, L., Sandy, D.A. & McKenzie, C.K. 1994. Blast damage mechanisms in open cut mining. In T.N. Little (ed.), *Proc. Open Pit Blasting Workshop 94*: 96–103. Perth, WA: Curtin Univ.

Ouchterlony, F., Sjöberg, C. & Jonsson, B.A. 1993. Blast damage predictions from vibration measurements at the SKB underground laboratories at Äspö in Sweden. *Proc. 9th Annual Symposium on Explosives and Blasting Research*: 189–197. Cleveland, OH: ISEE.

Ouchterlony, F. 1995. Review of rock blasting and explosives engineering research at SveBeFo. *Proc. Explo 95 Conference*: 133–146. Carlton, VIC: The AusIMM.

Sarma, K.S. 1994. Models for assessing the blasting performance of explosives. PhD thesis. Brisbane, QLD: Julius Kruttschnitt Mineral Research Centre, Univ. Queensland.

Siira, O. 1994. Economical consequences of cautious blasting/slope stability for the Aitik mine. In P. Andersson (ed.), *Skadezon vid Tunneldrivning*, SveBeFo rapport 8: 42–44. Stockholm: Swedish Rock Engineering Research.

Sognfors, P.-O. 1994. Cautious blasting of final slopes at the Aitik mine. *Proc. Blasting Conference*, paper no 13. Gyttorp: Nitro Nobel. In Swedish.